

Hydrothermal low-temperature preparation and characterization of ZnO nanoparticles supported on natural zeolite as a highly efficient photocatalyst

E. Sanatgar-Delshade · A. Habibi-Yangjeh ·
M. Khodadadi-Moghaddam

Received: 18 November 2009 / Accepted: 12 December 2010 / Published online: 14 January 2011
© Springer-Verlag 2011

Abstract Nanoparticles of zinc oxide were supported on natural zeolite using a hydrothermal method. The catalyst was characterized by X-ray diffraction, UV-vis diffuse reflectance spectra, scanning electron microscopy, and energy-dispersive X-ray techniques. The maximum rate constant for photodegradation of methylene blue (MB) was observed at 80 wt.% ZnO. The influence of various parameters such as catalyst composition, initial concentration of MB, calcination temperature, pH, and catalyst weight on the photodegradation reaction was studied. It was found that photodegradation of MB followed pseudo-first-order kinetics. The rate constant of the reaction for 80 wt.% ZnO at optimized conditions was approximately 3.8 times higher than that for bare ZnO. The photocatalyst had good reusability after four runs. The higher activity of the supported catalyst is due to greater adsorption of MB on the catalyst and its capability to delocalize the conduction-band electrons of excited ZnO.

Keywords Supported ZnO · Photocatalysis · Natural zeolite · Methylene blue · Nanoparticles

Introduction

Dyes and pigments are widely used in many industries for various purposes, and their effluents can cause

environmental pollution. Traditional techniques such as adsorption and coagulation by chemical agents are non-destructive and simply transfer the contaminant from water to another phase [1–3]. Photocatalysis, an advanced oxidation technology employing semiconductors as photocatalysts, is a promising method for treatment of contaminated ground, surface, and wastewater containing various organic pollutants [4–7]. This method is generally based on the generation of OH radicals, which interact with organic pollutants leading to progressive degradation and subsequently complete mineralization [8, 9]. Despite the positive attributes of photocatalysts, poor adsorption properties of semiconductors limit their application. To circumvent this limitation, several attempts have been made to improve the efficiency of photocatalysts by using suitable supports [10–14]. Among the various adsorbents, activated carbon has been applied as a commonly used support for TiO₂ and ZnO nanomaterials; for example, Li et al. [15] studied photocatalytic decolorization of methyl orange by TiO₂-coated activated carbon. In similar work, photodegradation of chromotrope 2R [16] and phenol [17] have been studied. Moreover, Sobana et al. [18] studied degradation of direct blue 53 and 4-acetylphenol [19] using ZnO supported on activated carbon. Although activated carbon has been the most widely used adsorbent, it suffers drawbacks of higher cost in production and regeneration [20].

Zeolites have more advantages owing to their special features such as high surface area, hydrophobic and hydrophilic properties, tunable chemical properties, high thermal stability, and ecofriendly nature [21]. As a typical porous material, zeolites can be divided into natural zeolites and synthetic zeolites. Synthetic and natural zeolites are important alternatives as adsorbents due to their high ion-exchange and adsorption capacities as well as their

E. Sanatgar-Delshade · A. Habibi-Yangjeh (✉)
Department of Chemistry, Faculty of Science,
University of Mohaghegh Ardabili, P.O. Box 179,
Ardabil, Iran
e-mail: ahabibi@uma.ac.ir

M. Khodadadi-Moghaddam
Department of Chemistry, Faculty of Science,
Islamic Azad University, Ardabil Branch, Ardabil, Iran

thermal and mechanical stabilities. The high cost of the support limits their extensive application in standard industry. For large-scale utilization, natural zeolites seem more appropriate than synthetic ones, due to their low cost, abundance, and less chemical pollution during production. Although there are extensive studies on the photocatalytic properties of TiO_2 supported on synthetic zeolites [22–26], studies on natural zeolite supports are rare. For example, Li et al. [27] studied photodegradation of methyl orange by TiO_2 supported on natural zeolite. Similarly, Nikazar et al. [13] investigated degradation of acid red 114 using TiO_2 supported on clinoptilolite in water. Also, there is only limited literature available on photocatalytic degradation of organic pollutants using ZnO supported on zeolite [28, 29]. Therefore, it is instructive to investigate the interaction between ZnO and natural zeolite as support to promote practical applications for environmental purpose.

For these reasons, in this work, preparation of ZnO supported on natural zeolite by low-temperature hydrothermal method was considered, and its photocatalytic activity towards photodegradation of methylene blue (MB), as a typical nonbiodegradable dye, was investigated. The influence of various parameters such as catalyst composition, initial concentration of MB, solution pH, weight of catalyst, and calcination temperature on the photodegradation rate constant was studied to achieve the maximum degradation efficiency. Moreover, photocatalyst reusability after four runs was determined.

Results and discussion

XRD patterns of samples with various ZnO loadings are illustrated in Fig. 1. For comparison, the XRD pattern of the pure natural zeolite is also shown in Fig. 1, being similar to that reported in literature [13]. The results reveal that the natural zeolite used in this work is mostly clinoptilolite. The XRD pattern for as-prepared ZnO nanoparticles is depicted in Fig. 1. All diffraction peaks for bare ZnO are in agreement with the JCPDS file for ZnO (JCPDS 36-1451), which can be indexed as a wurtzite hexagonal phase of ZnO with lattice constants of $a = b = 3.2498 \text{ \AA}$, and $c = 5.2066 \text{ \AA}$. No peaks attributable to possible impurities are observed. The sharp diffraction peaks show that the as-prepared ZnO nanoparticles had high crystallinity. The diffraction peaks correspond to (100), (002), (101), (102), (110), (103), (200), (112), (201), (004), and (202) planes of the ZnO crystal system. The XRD patterns of the supported catalysts indicate that coating of ZnO onto the adsorbent by the hydrothermal method did not change the structure of the support. Figure 1 clearly shows a gradual increase in the intensity of the peaks for ZnO and a corresponding decrease in the

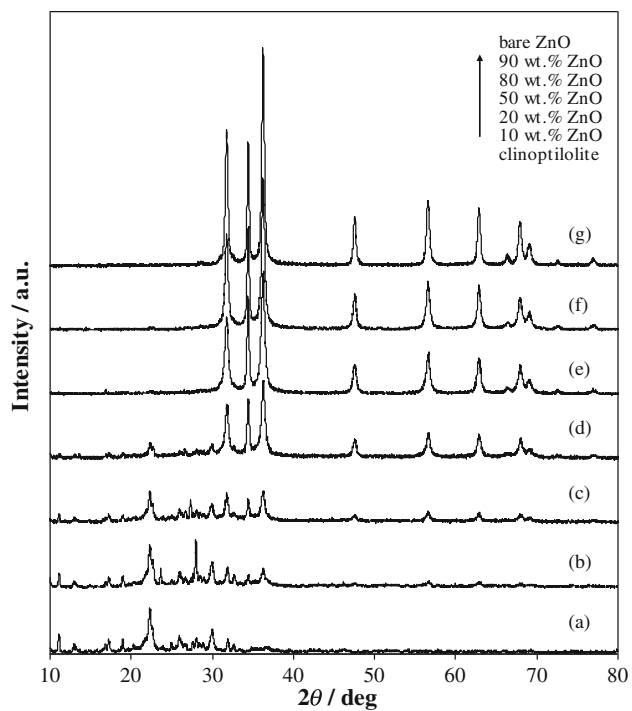


Fig. 1 Powder XRD patterns for *a* natural zeolite, *b* 10 wt.% ZnO , *c* 20 wt.% ZnO , *d* 50 wt.% ZnO , *e* 80 wt.% ZnO , *f* 90 wt.% ZnO , and *g* bare ZnO

intensity of peaks for the zeolite, indicating increasing ZnO loading on the photocatalyst. The average crystallite size, D , was calculated using Scherrer's equation [30]

$$D = K\lambda/(B\cos\theta), \quad (1)$$

where λ is the wavelength of X-ray radiation (0.15406 nm) used, K is Scherrer's constant ($K = 0.9$), θ is the characteristic X-ray radiation ($2\theta = 36.2^\circ$), and B is the full-width at half-maximum of the (101) plane (in radians). The crystallite size for as-prepared ZnO was 21.8 nm. Also, the particle size was 16.2, 16.4, 17.7, 18.7, and 18.9 nm for 10, 20, 50, 80, and 90 wt.% ZnO loading, respectively. Overall, the results indicate that the ZnO nanoparticle size increased with increasing ZnO loading, possibly due to aggregation of ZnO particles on the zeolite surface.

The morphology of the nanoparticles for as-prepared pure ZnO was investigated by scanning electron microscopy (SEM), as shown at various magnifications in Fig. 2. As can be seen, the ZnO nanoparticles were irregular nanoplates. Also, for comparison, SEM images of the natural zeolite are shown in Fig. 3. As can be seen, the particle size of the natural zeolite is mainly larger than 5 μm . The morphology of the supported catalysts was also investigated using SEM. The results indicated that the distribution of the ZnO nanoparticles on the surface of the zeolite increased with increasing ZnO loading. The ZnO

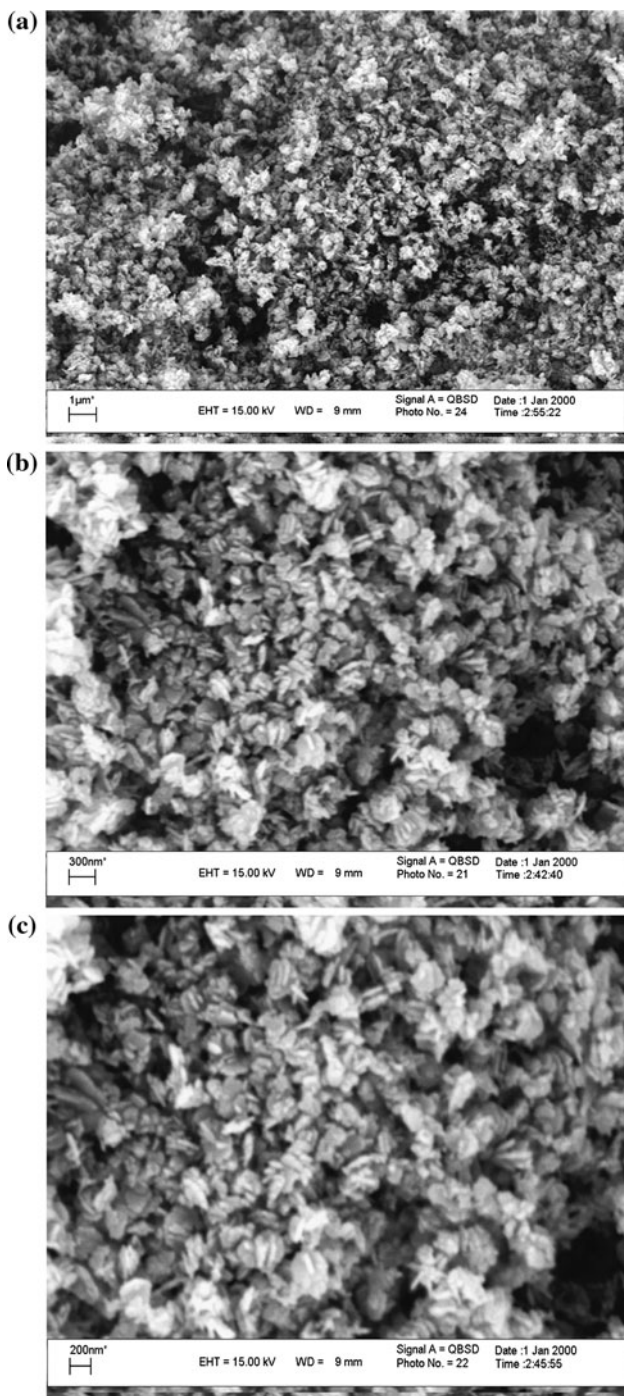


Fig. 2 SEM images of as-prepared ZnO nanoparticles at various magnifications

nanoparticles on the surface of the zeolite are clearly seen for higher ZnO loading (Fig. 4).

The purity and composition of the products were studied by using energy-dispersive X-ray spectroscopy (EDX, Fig. 5). The peaks were clearly related to the corresponding elements. Other peaks in this figure correspond to gold and palladium, which are due to sputter-coating of compounds on the EDX stage.

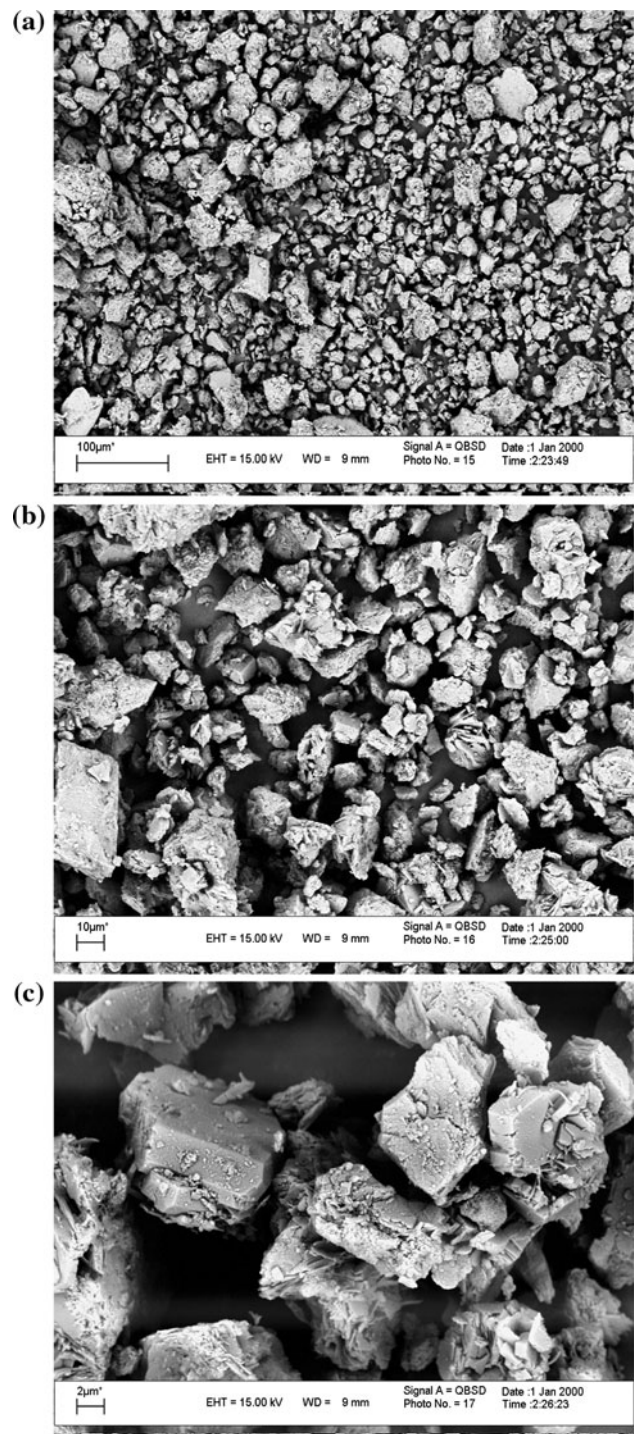


Fig. 3 SEM images of the natural zeolite at various magnifications

Figure 6 shows diffuse reflectance spectra (DRS) of the as-prepared ZnO, ZnO supported on the zeolite, and the natural zeolite. An absorption peak at about 320 nm was observed for the as-prepared nanoparticles of bare ZnO. This absorption wavelength is lower than that for bulk ZnO with absorption at 384 nm [31]. This can be attributed to

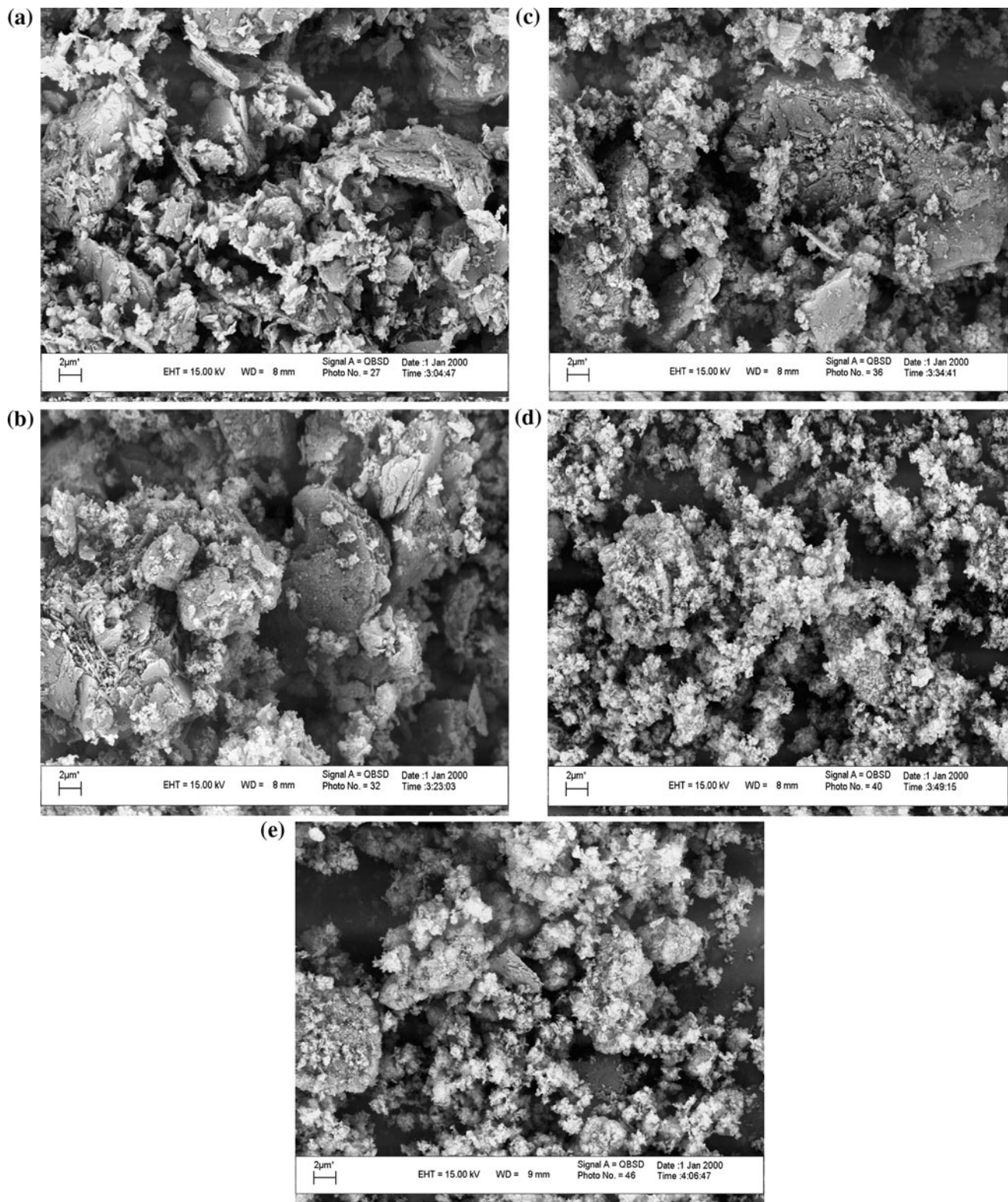


Fig. 4 SEM images of the as-prepared photocatalysts at various loadings of ZnO nanoparticles: **a** 10 wt.% ZnO, **b** 20 wt.% ZnO, **c** 50 wt.% ZnO, **d** 80 wt.% ZnO, and **e** 90 wt.% ZnO

the quantum confinement effect of the ZnO nanoparticles. In addition, DRS for the catalysts with various ZnO loadings on the zeolite are shown in Fig. 6. It is clear that there

is no remarkable change in absorption wavelength of the supported ZnO. As is known, the pore size of clinoptilolite is 0.4–0.7 nm [32], but the particle size of ZnO

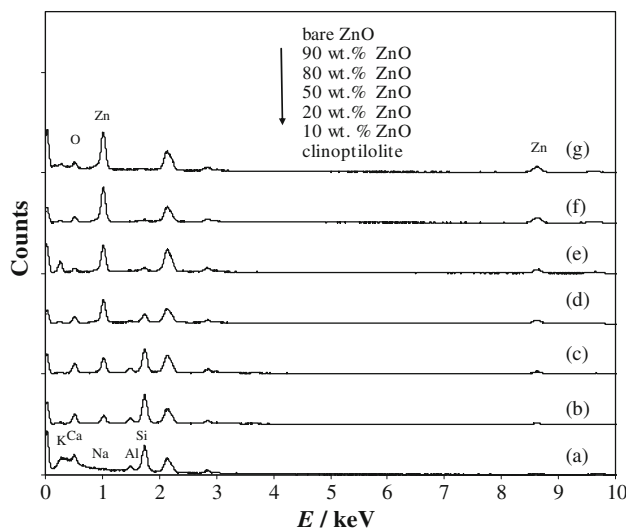


Fig. 5 EDX pattern of *a* natural zeolite, *b* 10 wt.% ZnO, *c* 20 wt.% ZnO, *d* 50 wt.% ZnO, *e* 80 wt.% ZnO, *f* 90 wt.% ZnO, and *g* bare ZnO

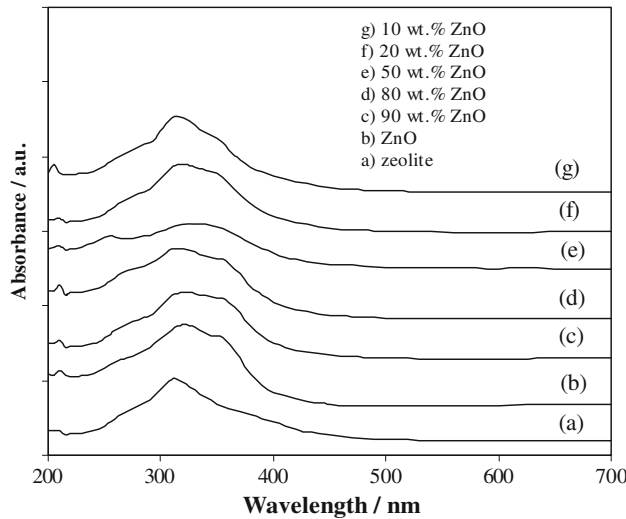


Fig. 6 Diffuse reflectance spectra (DRS) for *a* natural zeolite and *b* ZnO nanoparticles, along with the catalyst at various loadings: *c* 10 wt.% ZnO, *d* 20 wt.% ZnO, *e* 50 wt.% ZnO, *f* 80 wt.% ZnO, and *g* 90 wt.% ZnO

nano-particles calculated using Scherrer's equation is greater than 16 nm. Thus, the ZnO nano-particles were not able to enter the pores [32]. Therefore, we conclude that the ZnO nano-particles were loaded onto the surface of the zeolite instead of into the pores and cavities. ZnO nano-particles on the surface of the zeolite are clearly seen in the SEM images at various loadings (Fig. 4).

Photocatalytic degradation of MB was carried out in a batch reactor, and the reaction variables were optimized to obtain the maximum degradation efficiency. The essential reaction parameters (1) composition of the photocatalyst,

(2) calcination temperature, (3) catalyst weight, (4) initial MB concentration, and (5) pH were varied, and the results are described in the following sections.

Effect of composition of the supported photocatalyst

To understand the effect of catalyst composition on the photocatalytic degradation of MB, the ZnO loading on the catalyst was varied between 10 and 90 wt.%, and the results are shown in Fig. 7. All studies were carried out using 0.10 g catalyst and 1.70×10^{-5} M MB. For comparison, photolysis data (without any catalyst) are also shown in Fig. 7. It is clear that the photocatalyst composition has a remarkable effect on the photodegradation reaction of MB. In general, the dependence of the photocatalytic reaction rate on the concentration of organic pollutants is well described by the following kinetic model [33]:

$$\text{rate} = -\frac{d[\text{MB}]}{dt} = \frac{kK[\text{MB}]}{1 + K[\text{MB}]} \quad (2)$$

where k is the first-order rate constant of the reaction, K is the adsorption constant of the pollutant on the photocatalyst, $[\text{MB}]$ is the concentration of MB (mol/dm^3) at any time, and t is the irradiation time. Equation 2 can be simplified to a pseudo-first-order equation [33]:

$$\ln \frac{[\text{MB}]_0}{[\text{MB}]} = kKt = k_{\text{obs}}t \quad (3)$$

in which k_{obs} is the observed first-order rate constant of the photodegradation reaction. To examine whether the reaction rate could be congruent with a pseudo-first-order

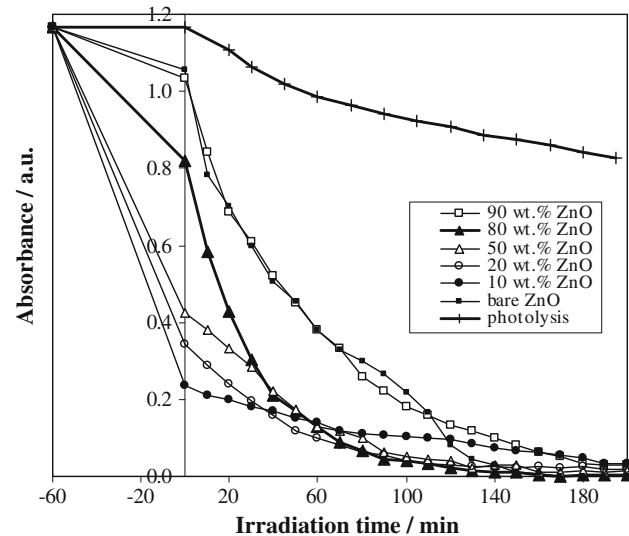


Fig. 7 Effect of photocatalyst composition on the photodegradation of MB (catalyst weight 0.10 g, $[\text{MB}] = 1.70 \times 10^{-5}$ M) along with photolysis data without any catalyst

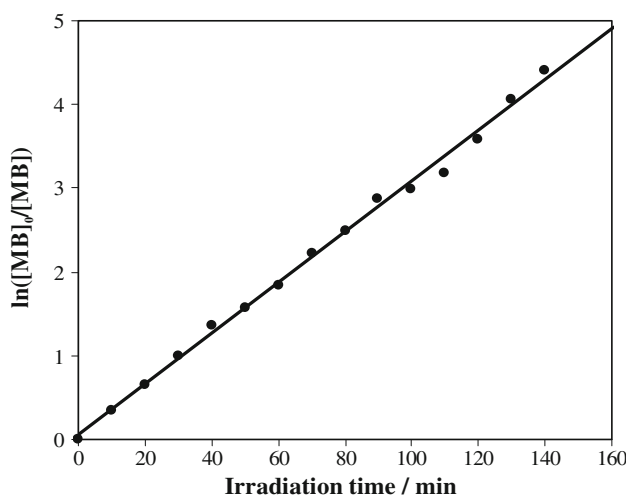


Fig. 8 Plot of $\ln([MB]_0/[MB])$ versus irradiation time for photodegradation of MB using the catalyst with 80 wt.% ZnO

reaction under different conditions, $\ln([MB]_0/[MB])$ was plotted against irradiation time for different ZnO loadings; for example, Fig. 8 shows a plot of $\ln([MB]_0/[MB])$ versus irradiation time for the catalyst with 80 wt.% ZnO. As can be seen, good linear correlation was found between $\ln([MB]_0/[MB])$ and irradiation time. To demonstrate the effect of ZnO loading on photocatalysis efficiency, values of k_{obs} at various ZnO loadings were obtained (Table 1). It is clear that the reaction rate constant increases with increasing ZnO loading on the photocatalyst, reaching a maximum at 80 wt.% ZnO. The photodegradation reaction rate is related to the formation of OH radical, which is the critical species in the degradation process [34]. It is clear that OH radical is produced on the ZnO nanoparticles. Thus, the reaction rate constant will increase with the ZnO loading of the photocatalyst. However, the produced OH radical is transferred onto the surface of the zeolite containing adsorbed MB (as organic pollutant), so the reaction rate decreases with increasing ZnO content after reaching a maximum (at 80 wt.% ZnO). Similar results have been reported for TiO₂ supported on natural zeolite [13]. This synergistic effect is attributed to the fact that the presence of the zeolite maintains the pollutant near the photocatalyst.

Table 1 Pseudo-first-order rate constant of the photodegradation reaction at various percentage ZnO loadings on the catalyst

No.	wt.% ZnO	$k_{\text{obs}} (\text{min}^{-1})$
1	100	0.0153
2	90	0.0190
3	80	0.0390
4	50	0.0224
5	20	0.0194
6	10	0.0115

Effect of calcination temperature

Generally, catalytic activity is dependent on the calcination temperature of the photocatalyst. It is accepted that higher calcination temperature causes formation of crystalline semiconductor on the support [35]. Therefore, it is expected that photocatalysts treated at higher temperatures might display better photocatalytic properties. The dependence of MB absorbance on irradiation time for various calcination temperatures is shown in Fig. 9. It is clear that the reaction rate constant increases with calcination temperature, reaches a maximum at 400 °C, and then decreases (Table 2). The decrease in the photocatalytic degradation rate for the catalyst treated at 500 °C may be due to aggregation of the ZnO nanoparticles. Similar results have been reported for various photocatalysts [35].

Effect of catalyst weight

Generally, the rate constant of the photocatalytic reaction depends on the catalyst weight [36, 37]. Hence, a series of experiments was carried out to find the optimum catalyst

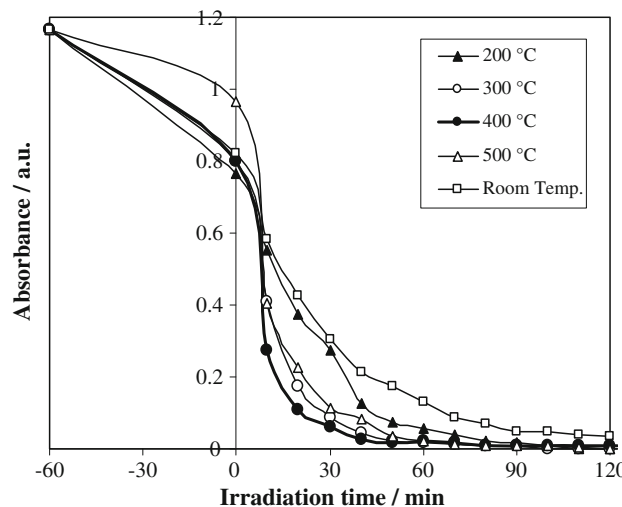


Fig. 9 Effect of calcination temperature on the photodegradation reaction of MB (catalyst composition 80 wt.% ZnO, catalyst weight 0.10 g, $[MB] = 1.70 \times 10^{-5}$ mol/dm³)

Table 2 Pseudo-first-order rate constant of the photodegradation reaction at various calcination temperatures of the catalyst

No.	Calcination temperature (°C)	$k_{\text{obs}} (\text{min}^{-1})$
1	Without calcination	0.0390
2	200	0.0453
3	300	0.0728
4	400	0.0749
5	500	0.0610

Table 3 Effect of catalyst weight on the rate constant of the photodegradation reaction (catalyst composition 80 wt.% ZnO, calcination temperature 400 °C, [MB] = 1.70×10^{-5} mol/dm³)

No.	Catalyst weight (g)	k_{obs} (min ⁻¹)
1	0.05	0.0418
2	0.1	0.0749
3	0.15	0.0784
4	0.2	0.0719
5	0.25	0.0655

amount by varying the photocatalyst weight between 0.05 and 0.25 g (Table 3). As can be seen, the photodegradation rate constant increased with increasing photocatalyst weight, and then decreased. A maximum value was achieved at 0.15 g photocatalyst, which might be due to two competing processes [36]. In general, the greater the amount of photocatalyst, the higher the reaction rate should be, due to the fact that active sites of the photocatalyst are increased. However, more photocatalyst would also induce greater aggregation of the photocatalyst and reduce its specific surface area, leading to a reduction in the reaction rate. Also, this might be due to scattering of light and reduction in light penetration through the solution [38].

Effect of initial MB concentration

The pollutant concentration is an important parameter in wastewater treatment [16, 39]. The effect of initial MB concentration on the degradation rate was studied by varying the initial concentration between 8×10^{-6} and 2.4×10^{-5} M for constant catalyst weight of 0.15 g, and the k_{obs} values were calculated (Table 4). It is clear that the photodegradation rate decreases with increasing initial concentration of MB. When the initial concentration increases, more organic substances are adsorbed on the surface of the photocatalyst. Therefore, there are fewer active sites for adsorption of hydroxyl ions, so generation of hydroxyl radicals will be reduced. The photodegradation reaction rate is related to the formation of OH radical [34], so the photodegradation rate constant decreases with the

Table 4 Effect of initial concentration of MB on the reaction rate constant (catalyst composition 80 wt.% ZnO, weight 0.15 g, calcination temperature 400 °C)

No.	Concentration (10^{-5} mol/dm ³)	k_{obs} (min ⁻¹)
1	0.8	0.1268
2	1.1	0.0856
3	1.7	0.0784
4	2.4	0.0459

concentration of MB. Furthermore, as the concentration of MB increases, photons are intercepted before they can reach the catalyst surface and the screening effect dominates, preventing penetration of the light to the photocatalyst, hence adsorption of photons by the catalyst decreases and consequently the degradation rate is reduced [39, 40].

Effect of solution pH

The initial pH of a solution influences the adsorption and dissociation of substrate, the catalyst surface charge, the oxidation potential of the valence band, and other physicochemical properties of the system [41]. Thus, solution pH is an important variable in aqueous-phase-mediated photocatalytic reactions. The effect of pH on the rate constant of photocatalytic degradation by supported and unsupported ZnO was studied by keeping all other experimental conditions constant and varying the initial pH of the MB solution from 1.5 to 10. The solution pH was adjusted only prior to irradiation and not controlled during the reaction, and the results are depicted in Fig. 10. Obviously photocatalytic degradation of MB by supported and unsupported ZnO was favored in alkaline pH. The degradation reaction rate constant using supported ZnO suddenly increases with increasing pH (Table 5). To demonstrate the effect of adsorption extent of MB on the reaction rate constant using supported ZnO, the adsorption extent of MB was plotted versus the pH of the solution (Fig. 11). It is clear that adsorption of MB on the supported ZnO increases with pH. The increase in the degradation rate with increasing pH of the solution would be due to increased adsorption of MB on the surface of the catalyst. The zero point charge pH for ZnO is 9 [42]. Above this

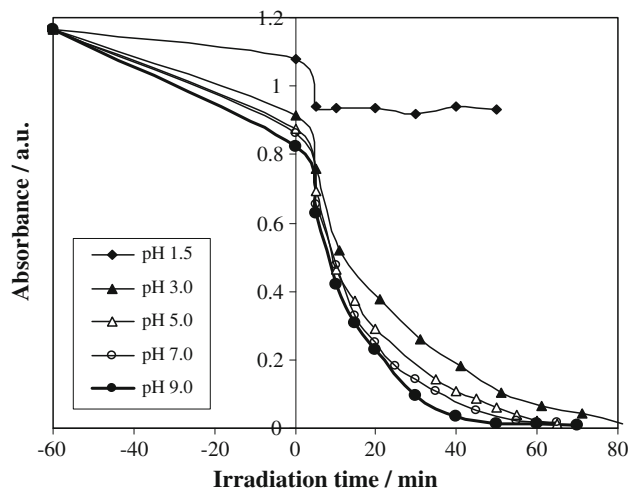
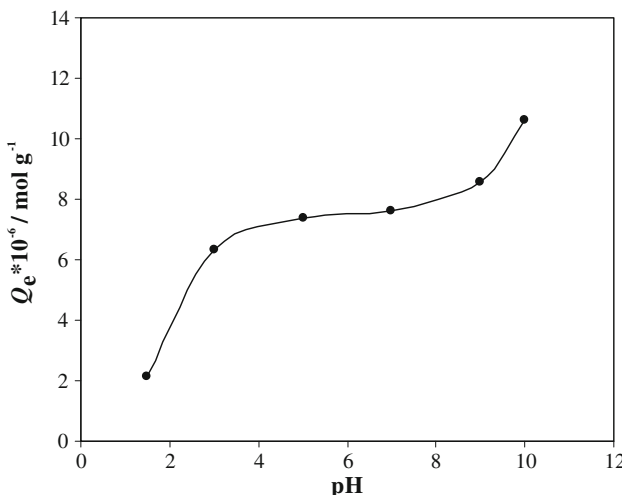


Fig. 10 Effect of solution pH on the photodegradation of MB (catalyst composition 80 wt.% ZnO, weight 0.15 g, calcination temperature 400 °C, [MB] = 1.70×10^{-5} mol/dm³)

Table 5 Pseudo-first-order rate constant for photodegradation of MB using ZnO and ZnO/zeolite at various pH values

No.	pH	k_{obs} (min ⁻¹) (for ZnO)	k_{obs} (min ⁻¹) (for ZnO/zeolite)
1	1.5	0.0008	0.0016
2	3	0.0144	0.0453
3	5	0.0147	0.0509
4	7	0.0153	0.0784
5	9	0.0222	0.0851
6	10	0.0310	0.0942

**Fig. 11** Effect of solution pH on adsorption extent of MB on the catalyst with 80 wt.% ZnO at 25 °C

value, the ZnO surface is negatively charged by means of adsorbed OH⁻. At pH below the zero point charge of ZnO, the catalyst is mainly positively charged. In alkaline solution, electrostatic interactions between MB with cationic charge and ZnO (also zeolite) with anionic charge would favor adsorption of the dye, so photodegradation efficiency will be favored by increasing pH. Also, the presence of large quantities of OH⁻ ions on the photocatalyst surface favors the formation of OH radical, which is accepted as the primary oxidizing species responsible for photodegradation [34].

In contrast, at low pH, the ZnO surface is positively charged and repulsive forces between the photocatalyst and the cationic dye will lead to a decrease in dye adsorption and the photodegradation rate. Furthermore, the ZnO nanoparticles have a tendency to dissolve with decreasing pH of the solution [43]:



Therefore, in acidic solution, the photocatalyst has low stability and so the photocatalytic reaction rate decreases suddenly with pH.

Table 6 Degradation percentage of MB on supported ZnO at optimized conditions in various runs

Number of runs	Degradation (%)
1	100
2	98
3	95
4	88

Photocatalyst reusability

Photocatalyst reusability is a very important parameter to obtain high efficiency. To determine the reusability of the catalyst, photodegradation experiments were carried out in optimized conditions (catalyst composition 80 wt.% ZnO, calcination temperature 400 °C, catalyst weight 0.15 g, [MB] = 1.70 × 10⁻⁵ mol/dm³, pH 9), and the results are presented in Table 6. In each experiment, the photocatalyst was recycled after filtrating and heating at 550 °C for 2 h. It can be seen that the degradation decreases to 88% after four runs, indicating that the photocatalytic activity has good repeatability. The decrease of the degradation percentage is explained by adsorption of organic intermediates and by-products of photodegradation in the cavities and on the surface of the photocatalyst that influence the surface activity of the catalyst [44]. Moreover, heat treatment will increase the photocatalyst aggregation after several runs, resulting in decreased surface area and finally leading to decreased photocatalytic efficiency [14].

In addition, SEM images of fresh and used photocatalyst were studied (Fig. 12). As can be seen, the SEM images for the fresh and used photocatalyst are similar to each other. For this reason, the photocatalyst is reusable for more runs without losing its activity.

Comparison of photocatalytic activity of ZnO and ZnO/zeolite

To demonstrate the effects of the natural zeolite on the photocatalytic properties of ZnO, photodegradation experiments were carried out by supported and unsupported ZnO under optimized conditions (catalyst composition 80 wt.% ZnO, calcination temperature 400 °C, catalyst weight 0.15 g, [MB] = 1.70 × 10⁻⁵ mol/dm³, pH 9). The results revealed that bare ZnO requires approximately 160 min for complete degradation of MB whereas ZnO/zeolite requires only 52 min (Fig. 13). Also, the rate constant for photodegradation of MB using the catalyst with 80 wt.% ZnO was approximately 3.8 times greater than that using bare ZnO. The higher efficiency of the photocatalyst can be attributed to the greater adsorption of MB on the photocatalyst. The adsorption capacity of the

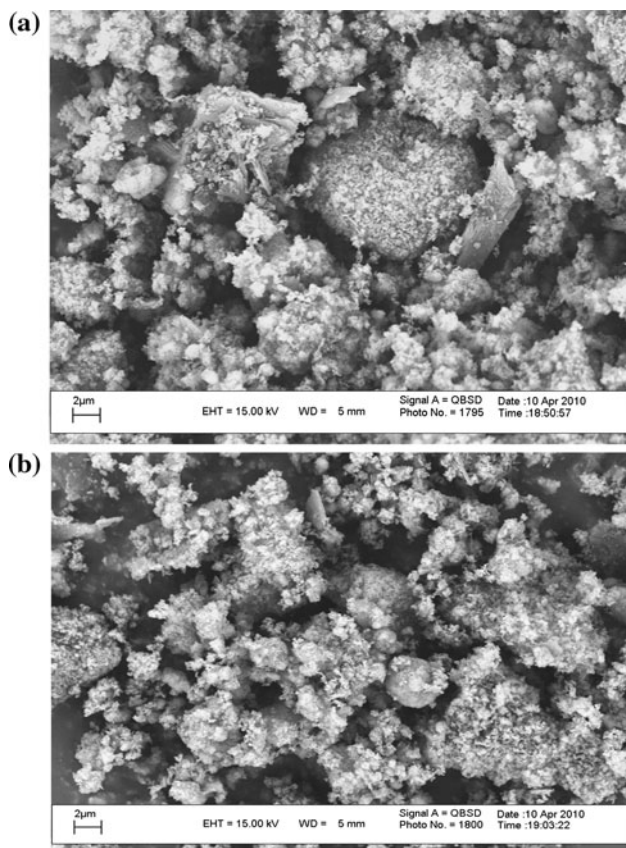


Fig. 12 SEM images for **a** fresh and **b** used photocatalysts

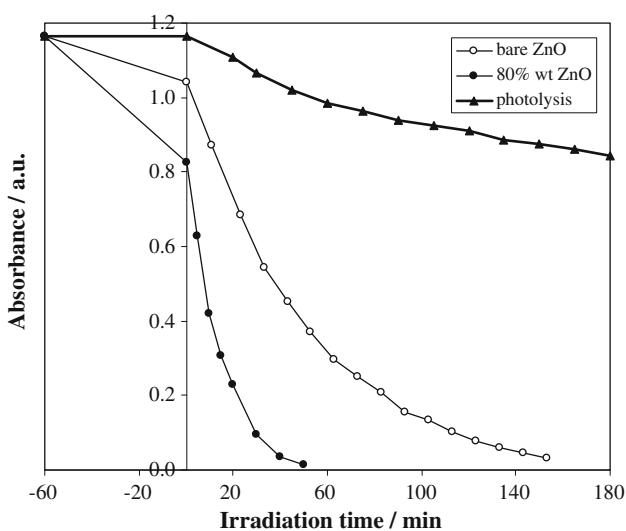


Fig. 13 Photodegradation of MB using supported and unsupported ZnO nanoparticles (catalyst composition 80 wt.% ZnO, calcination temperature 400 °C, [MB] = 1.70×10^{-5} mol/dm 3 , catalyst weight 0.15 g, pH 9) along with photolysis without any catalyst

zeolite enhances the chance of OH radicals attacking the adsorbed MB, resulting in faster degradation. Also, the delocalization capacity of the zeolite framework can

efficiently separate the electrons and holes produced during photoexcitation of ZnO, thus enhancing the photocatalytic efficiency.

Conclusions

A hydrothermal low-temperature method was proposed for preparation of ZnO nanoparticles on natural zeolite as a highly efficient photocatalyst. The method has advantages over other processes because of its simplicity and low equipment cost. The rate constant for photodegradation reaction and adsorption of MB on the catalyst increased with increasing pH of the solution. A catalyst amount of 0.60 g/dm 3 was found to be optimum for better degradation. The supported photocatalyst with 80 wt.% ZnO loading on the zeolite exhibited a rate constant approximately 3.8 times greater than bare ZnO for degradation of MB. Complete degradation of MB was observed within 52 min for the ZnO/zeolite system compared with 160 min for bare ZnO.

Materials and methods

Materials

Natural zeolite was commercial clinoptilolite (CP) (Afrand Tuska, Iran) from deposits in the region of Semnan. All other reagents were of analytical grade and used without further purification. The raw zeolite was washed with double-distilled water and then dried at 50 °C for 24 h. All of the resultant natural zeolite was kept in desiccator until synthesis of ZnO/zeolite.

Instruments

X-ray diffraction (XRD) patterns were recorded on a Philips Xpert X-ray diffractometer using Cu K α radiation ($\lambda = 0.15406$ nm), employing scanning rate of 1°/min in the 2 θ range from 10° to 80°. Surface morphology and distribution of particles were studied via LEO 1430VP scanning electron microscope (SEM), using accelerating voltage of 15 kV. The purity determination and elemental analysis of the products were carried out by energy-dispersive X-ray (EDX) analysis on the same LEO 1430VP instrument with accelerating voltage of 20 kV. For SEM and EDX, samples were mounted on an aluminum support using double adhesive tape and coated with a thin layer of gold and palladium. Diffuse reflectance spectra (DRS) were recorded by a Scinco 4100 apparatus.

Preparation of photocatalyst

The catalyst supported on natural zeolite was prepared with different ZnO loadings (10, 20, 50, 80, and 90 wt.%). In a typical synthesis procedure, 5.38 g zinc acetate dihydrate was dissolved in 25 cm³ double-distilled water, and then 2.0 g zeolite was added under stirring at room temperature. After 12 h stirring, aqueous solution of NaOH (5 M) was slowly added dropwise to the solution under magnetic stirring. Addition of NaOH was continued until the pH of the solution reached 13. The formed white precipitates were refluxed at approximately 95 °C for 120 min. The precipitate was centrifuged and washed twice with double-distilled water and ethanol, respectively, to remove unreacted reagents and dried in an oven at 50 °C. For comparison of the photocatalytic properties of unsupported ZnO with supported nanoparticles, nanoparticles of bare ZnO were prepared by a similar method to that mentioned above.

Photocatalysis and adsorption experiments

To examine the photocatalytic activity of the catalysts, photodegradation of methylene blue (MB), which is a typical nonbiodegradable dye, was investigated. A photochemical reactor provided with a water circulation arrangement to maintain temperature at 25 °C was used in the experiments. The initial pH of the solution was maintained by adding HCl or NaOH. The solution was magnetically stirred and continuously aerated by a pump to provide oxygen and complete mixing of the reaction solution. An ultraviolet (UV) lamp (125 W) with the major fraction of irradiation at 365 nm was used. Prior to illumination, a suspension containing 0.05–0.25 g photocatalyst and 250 cm³ MB (8×10^{-6} – 2.4×10^{-5} M) was stirred continuously in the dark for 1 h, to attain adsorption equilibrium. Samples were taken from the reactor at regular intervals and centrifuged to remove the catalyst before analysis by spectrophotometer at 664 nm, corresponding to the maximum absorption wavelength (λ_{\max}) of MB. The prepared photocatalysts were stored in a desiccator to prevent moisture adsorption and to retain photocatalytic activity. The extent of adsorption of MB on the catalyst (Q_e , mol/g) was calculated by Eq. 5:

$$Q_e = \frac{(C_0 - C_e)V}{W}, \quad (5)$$

where C_0 and C_e are the initial and equilibrium concentration of the dye in solution, respectively, V is the volume of working solution (dm³), and W is the weight of the photocatalyst.

Acknowledgments The authors wish to acknowledge the vice-presidency of research, University of Mohaghegh Ardabili, for financial support of this work.

References

- Ozdemir O, Armagan B, Turan M, Celik MS (2004) Dyes Pigment 62:49
- Wang S, Li H, Xie S, Liu S, Xu L (2006) Chemosphere 65:82
- Selvam PP, Preethi S, Basakaralingam P, Thinakaran N, Sivasamy A, Sivanesan S (2008) J Hazard Mater 155:39
- Gogate PR, Pandit AB (2004) Adv Environ Res 8:501
- Kabra K, Chaudhary R, Sawhney RL (2004) Ind Eng Chem Res 43:7683
- Reddy MP, Venugopal A, Subrahmanyam M (2006) Appl Catal B Environ 69:164
- Dalrymple OK, Yeh DH, Trotz MA (2007) J Chem Technol Biotechnol 82:121
- Wu C-H, Chern J-M (2006) Ind Eng Chem Res 45:6450
- Teichner SJ (2008) J Porous Mater 15:311
- Zhao X, Lu G, Millar GJ (1996) J Porous Mater 3:61
- Khouchaf L, Tuilier MH, Wark M, Soulard M, Kessler H (1998) Microporous Mesoporous Mater 20:27
- Xia H, Tang F (2003) J Chem Phys B 107:9178
- Nikazar M, Gholivand K, Mahanpoor K (2008) Desalination 219:293
- Huang M, Xu C, Wu Z, Huang Y, Lin J, Wu J (2008) Dyes Pigment 77:327
- Li Y, Li X, Li J, Yin J (2006) Water Res 40:1119
- Wang W, Silva CG, Faria JL (2007) Appl Catal B Environ 70:470
- Liu SX, Chen XY, Chen X (2007) J Hazard Mater 143:257
- Sobana N, Swaminathan M (2007) Solar Energy Mater Solar Cells 91:727
- Sobana N, Muruganandam M, Swaminathan M (2008) Catal Commun 9:262
- Wang SB, Boyjoo Y, Choueib A, Zhu ZH (2005) Water Res 39:129
- Corma A (1997) Chem Rev 97:2373
- Shankar MV, Cheralathan KK, Arabindoo B, Palanichamy M, Murugesan V (2004) J Mol Catal A Chem 223:195
- Bhattacharyya A, Kawi S, Ray MB (2004) Catal Today 98:431
- Mohamed RM, Ismail AA, Othman I, Ibrahim IA (2005) J Mol Catal A Chem 238:151
- Yoon S-J, Lee YH, Cho WJ, Koh IO, Yoon M (2007) Catal Comm 8:1851
- Li G, Zhao XS, Ray MB (2007) Sep Purif Technol 55:91
- Li F, Jiang Y, Yu L, Yang Z, Hou T, Sun S (2005) Appl Surface Sci 252:1410
- Anandana S, Vinub A, Venkatachalam N, Arabindo B, Murugesan V (2006) J Mol Catal A Chem 256:312
- Wang L, Wu H, Xu J, Li L (2008) Adv Composites Lett 17:187
- Cullity BD (1978) Elements of X-ray diffraction, 2nd edn. Addison Wesley, London
- Berger LI (1997) Semiconductor materials. CRC Press, Boca Raton
- Li F, Jiang Y, Yu L, Yang Z, Hou T, Sun S (2005) Appl Surface Sci 252:1410
- Behnajady MA, Modirshahla N, Hamzavi R (2006) J Hazard Mater B 133:226
- Shankar MV, Neppolian B, Sakthivel S, Arabindoo MB, Palanichamy M, Murugesan V (2001) Ind J Eng Mater Sci 8:104
- Wang C-C, Lee C-K, Lyu M-D, Juang L-C (2008) Dyes Pigment 76:817

36. Zhang L, Liu CY, Ren XM (1995) *J Photochem Photobiol A Chem* 85:239
37. Sakthivel S, Neppolian B, Shankar MV, Arabindoo B, Palanichamy M, Murugesan V (2003) *Sol Energy Mater Sol Cells* 77:65
38. Daneshvar N, Salari D, Khataee AR (2003) *J Photochem Photobiol A Chem* 157:111
39. Chakrabarti S, Dutta BK (2004) *J Hazard Mater B* 112:269
40. Daneshvar N, Aber S, Seyed Dorraji MS, Khataee AR, Rasoulifard MH (2007) *Sep Purif Technol* 58:91
41. Shankar MV, Anandan S, Venkatachalam N, Arabindoo B, Murugesan V (2004) *J Chem Technol Biotechnol* 79:1279
42. Sobana N, Swaminathan M (2007) *Sep Purif Technol* 56:101
43. Daneshvar N, Salari D, Khataee AR (2004) *J Photochem Photobiol A Chem* 162:317
44. Subba-Rao KV, Subrahmanyam M, Boule P (2004) *Appl Catal B Environ* 49:239